

Available online at www.sciencedirect.com**ScienceDirect**

Energy Procedia 69 (2015) 24 – 33

Energy
Procedia

International Conference on Concentrating Solar Power and Chemical Energy Systems,
SolarPACES 2014

Transient characterization of multiple parabolic trough collector loops in a 100 MW CSP plant for solar energy harvesting

A. Almasabi^a, A. Alobaidli^b, T.J. Zhang^{*a}

^a*Department of Mechanical and Materials Engineering,*

Masdar Institute of Science and Technology, P. O. Box 54224, Abu Dhabi, UAE

^b*Shams Power Company, P. O. Box 54114, Abu Dhabi, UAE*

Abstract

Parabolic trough solar collection technology has been widely deployed in concentrated solar power (CSP) generation plants all over the world. In a large-scale CSP plant, a solar field consists of hundreds of parabolic solar collector loops. Due to the parallel loop arrangement (Fig. 1) and non-uniform solar collection, mal-distributions of heat-transfer-fluid flow (HTF, synthetic oil) among different loops commonly occur during transient operation. Many solar collector loops have to be pushed out of tracking phase to avoid oil overheating and degradation, which causes significant loss in solar energy collection and power generation. Such collector defocusing and refocusing operation results in large transient variation of HTF temperature, which further brings challenges to energy-efficient operation and maintenance of the coupled thermal power generation unit. Advanced transient analysis, control and fault diagnosis tools are desired to achieve safer CSP plant operation and transient solar power harvesting. In this paper, a distributed transient optical-thermal-fluid model of parabolic trough collector is developed and validated with field data from a 100MW_{th} CSP plant. Transient model predictions are in fair agreement with experimental field data, which provide a quantitative tool for solar energy harvesting. Conceptual active flow control strategies are further introduced to regulate the HTF temperature and maintain high solar collection efficiency.

© 2015 The Authors. Published by Elsevier Ltd. This is an open access article under the CC BY-NC-ND license (<http://creativecommons.org/licenses/by-nc-nd/4.0/>).

Peer review by the scientific conference committee of SolarPACES 2014 under responsibility of PSE AG

Keywords: Parabolic Trough Collector, Distributed Modeling, Transient, Solar Energy Harvesting

* Corresponding author. Tel.: +971-2-810-9424; fax: +971-2-810-9901.

E-mail address: tjzhang@masdar.ac.ae

1. Introduction

Concentrating solar power technologies (CSP) have been accepted as one of the promising renewable energy technologies for large-scale power generation [1-3]. As a great example of diversifying the energy mix with renewable energy, the largest Concentrating Solar Power (CSP) plant in the Middle East and North Africa (MENA), Shams 1, was recently launched in Abu Dhabi, UAE. Shams 1 CSP plant consists of 192 parallel parabolic trough solar collector loops and an integrated with a Rankine power cycle (Fig. 1). The aim of the Shams 1 project was to build a CSP plant in MENA's harsh environment (i.e., wind, sand, water scarcity) while still maintaining efficiencies comparable to or better than conventional CSP plants in Europe and USA. Moreover, parabolic trough solar collectors are widely used for other applications, such as heating, cooling, and desalination [4, 5].

In fact, significant challenges are also associated with high investment cost and relatively low efficiency of CSP technologies [1-2], which are limiting their wide deployment. Therefore, innovation becomes critical to make large-scale CSP technologies more competitive and successful [3]. It is essential to develop advanced solar energy harvesting technologies for parabolic trough CSP plants. In order to characterize the unsteady parabolic trough solar collector loop, a dynamic model was developed in [6] for automatic control and operation purposes. An energy-based distributed control approach was proposed to regulate the loop exit HTF (oil) temperature [7]. In order to apply the feedback linearization control, the dynamics of solar field was approximated by a simplified lumped-parameter nonlinear model in [8]. In fact, all these studies were limited to single solar collector loop. For multiple parallel solar collector loops, it is not trivial to maintain uniform HTF exit temperature. Entropy would generate from the multi-loop HTF mixing process in the hot header. To our best knowledge, no one has investigated the solar radiation loss because of the swinging of parabolic trough collectors in large-scale solar fields. Based on our preliminary analysis, this has great potential of enhancing the solar thermal energy conversion efficiency.

Our ultimate goal is to develop a multipurpose toolbox for advanced CSP plant design, optimization, fault diagnosis and operator training. In this paper, we focus on the transient characterization of the 100 MWth Shams-1 parabolic trough CSP Plant. Through close collaboration with the Shams Power Company, we have collected massive field data to validate transient component and plant models, which will eventually become the core tool to harvest transient solar energy through active CSP plant control. The anticipated transient CSP simulator and control system can even be used for training the operators to deal with extreme CSP plant operations.

Nomenclature

| | |
|----------|---|
| D_i | Inner diameter of the receiver (m) |
| D_o | Receiver outer diameter (m) |
| t | Time (s) |
| A_w | Receiver cross section Area (m^2) |
| A_f | Fluid cross section area (m^2) |
| T_a | Ambient temperature ($^{\circ}C$) |
| T_w | Receiver wall temperature ($^{\circ}C$) |
| T_f | Fluid temperature ($^{\circ}C$) |
| ρ | Density (kg/m^3) |
| C_p | Specific heat at constant pressure (J/kg K) |
| k | Thermal conductivity (W/m K) |
| H_t | Heat transfer coefficient ($W/(m^2 K)$) |
| H_l | Total heat loss to surrounding (W/m) |
| DNI | solar irradiance (W/m^2) |
| G | Collector aperture (m) |
| η_o | Collector efficiency |
| A_v | Valve opening percentage |
| HTF | Heat transfer fluid |

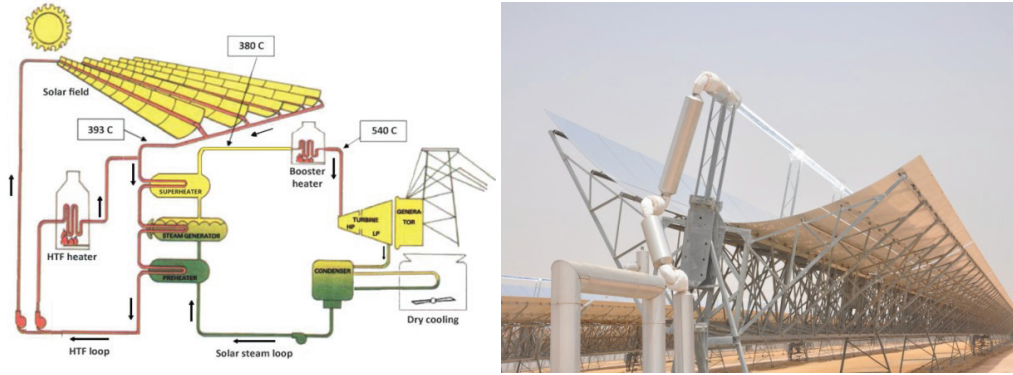


Fig. 1 (a) Diagram of a 100-MW concentrating solar thermal power plant (b) Photo of a parabolic trough solar collector loop at Shams-1 CSP plant in UAE

2. Characteristics of solar collector loops

In large commercial solar plants, solar collection performance and energy quality would affect the operational efficiency and lifetime of the coupled thermal power generation unit. In order to maximize transient solar power production, characteristics of parabolic trough collector loops must be quantified by considering the fluctuations in environmental conditions, such as DNI, wind speed, ambient temperature.

In such a 100 MW CSP plant, each HTF loop consists of four parabolic trough collectors, as seen in Fig. 2. At the middle of each collector, there exist a thermocouple providing the HTF temperature measurement. Each loop exit temperature is monitored to avoid the HTF overheating and degradation.

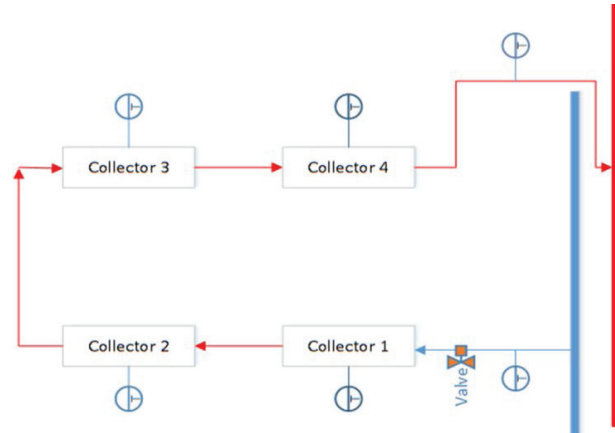


Fig. 2 Typical layout of parabolic trough solar collector loop

These long solar collector tubes exhibit distributed thermal-fluid characteristics. From the thermocouple readings, significant HTF temperature rises have been observed from the loop inlet to the loop exit.

A 1-dimensional energy conservation law is applied to the solar receiver wall (illustrated in Fig. 3):

$$\frac{\partial}{\partial t}(\rho_w A_w C_p T_w) = \frac{\partial}{\partial x} \left(k_w A_w \frac{\partial T_w}{\partial x} \right) + DNI n_o G - \pi D_o h_l (T_w - T_a) - \pi D_i H_t (T_w - T_f) \quad (1)$$

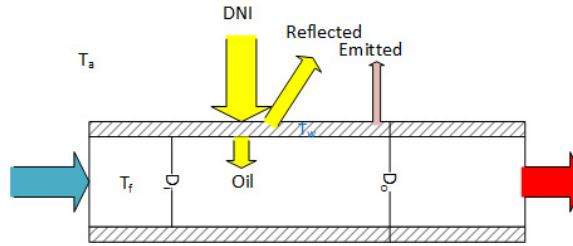


Fig.3 Diagram of a solar receiver tube

In Eq.(1.1), the transient wall heat storage is represented by the axial heat conduction and solar heat absorption by wall surface as well as the heat loss to the surrounding and convection heat transfer to the working fluid (HTF oil).

The heat loss of Schott's PTR70 receiver to the surrounding has been characterized by F. Burkholder and C. F. Kutscher in [9]

$$H_l = A_0 + A_1(T_f - T_a) + A_2T_f^2 + A_3T_f^3 + A_4 I K T_f^2 + \sqrt{V_{wind}} (A_5 + A_6(T_f - T_a)) \quad (2)$$

where A_0 to A_6 are constants coefficient can be found in [9].

The incident angle modifier [9]

$$K = \min(1, \cos(\theta_{deg}) + 0.000884 \theta_{deg} - 0.00005369 \theta_{deg}^2) \quad (3)$$

In a same manner, the energy balance is also applicable to the HTF, Thermol VP1 synthetic oil, in the receiver tubes

$$\frac{\partial}{\partial t}(\rho_f A_f u_f) = \frac{\partial}{\partial x} \left(k_f A_f \frac{\partial T_f}{\partial x} \right) - \frac{\partial}{\partial x}(\dot{m}_f h_f) + \pi D_i H_t (T_w - T_f) \quad (4)$$

In order to model the distributed thermal-fluidic transients, the method of lines is applied to the partial differential equations (1.1)-(1.2) by discretizing the spatial derivatives with finite difference. As a result, a set of coupled ordinary differential equations are formulated in terms of the time derivatives:

$$\frac{dT_w^j}{dt} = \frac{k_w A_w \frac{T_w^{j+1} + T_w^{j-1} - 2T_w^j}{\Delta x^2} + I n_o G - H_l - \pi D_i H_t (T_w^j - T_f^j)}{\rho_w A_w C_{p_w}} \quad (5)$$

$$\frac{dT_f^j}{dt} = \frac{\rho_f \dot{q} \frac{cp_f^{j-1} T_f^{j-1} - cp_f^j T_f^j}{\Delta x} + \pi D_i H_t (T_w^j - T_f^j)}{\rho_f A_f \left(cp_f + T_f \left(\frac{dcp_f}{dT} \right) \right)} \quad (6)$$

With the Matlab ODE15s, transient behavior of solar receiver tube and HTF can be predicted. As seen from Eqs.(1.5)-(1.6), the temperatures of the oil and tube walls are coupled during simulation.

3. Transient characterization results

Solar field data were collected on June 24 and 25, 2014 from 7am to 6 pm. Here we focus on two solar collector loops. Both of them were dirty on June 24 and cleaned on June 25. Figs. 4-5 and Figs. 8-9 show the ambient temperature, wind speed, loop inlet flow rate and direct normal irradiance (DNI) on these two days. The DNI for the second day is higher, which required higher inlet HTF flow rate. The inlet valve opening positions for the two loops were kept constant: 60% for Loop 1 and 51% for Loop 2. As seen from Fig. 10, there are three typical modes of operations: Tracking (2), out-focus (3) and partial out-focus (12). The last one is 30 percent out-of-tracking. It can be seen from Figs. 6-7 and Fig. 10 that the HTF temperature is highly affected by the operation mode of solar collector (Fig. 11). The CSP plant operators usually change the tracking mode of solar collectors to regulate HTF temperature.

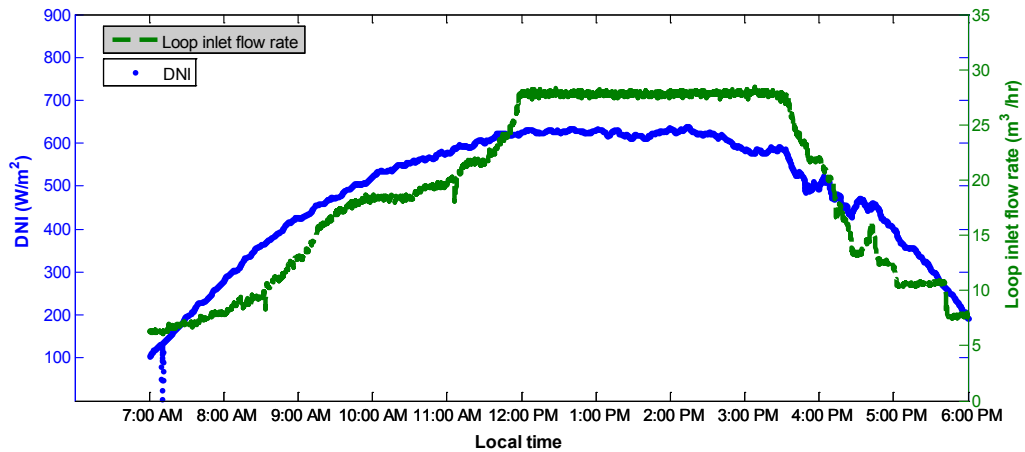


Fig. 4 Transient loop inlet flow rate (dashed line) and DNI (blue dot) on June 24, 2014 during 7am-6pm

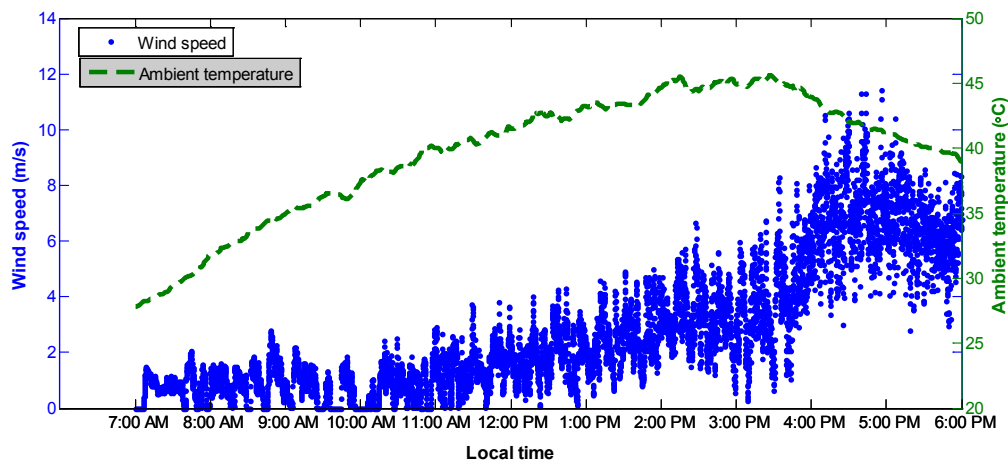


Fig. 5 Transient ambient temperature (dashed line) and wind speed (blue dots) on June 24, 2014 during 7am-6pm

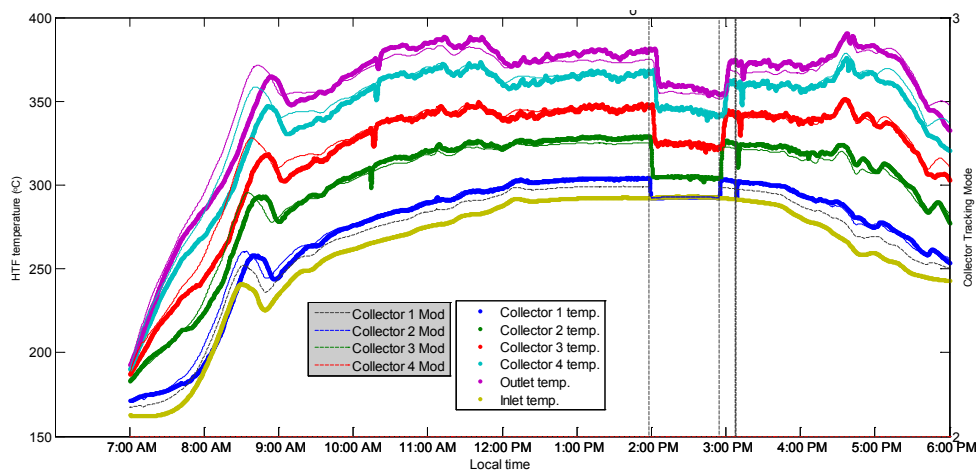


Fig. 6 Transient Loop 1 HTF temperature, exit temperature and operation mode on June 24, 2014 during 7am-6pm (thin solid line: model prediction; thick dashed line: measurement)

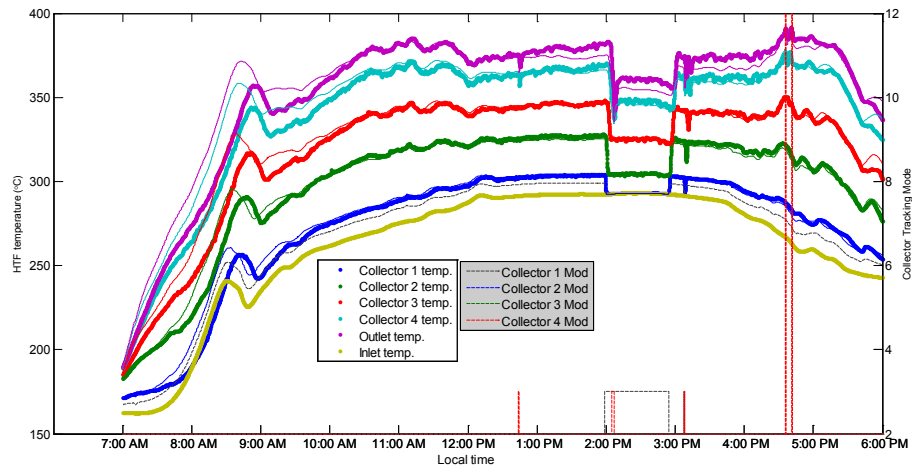


Fig. 7 Transient Loop 2 HTF temperature, exit temperature and operation mode on June 24, 2014 during 7am-6pm (thin solid line: model prediction; thick dashed line: measurement)

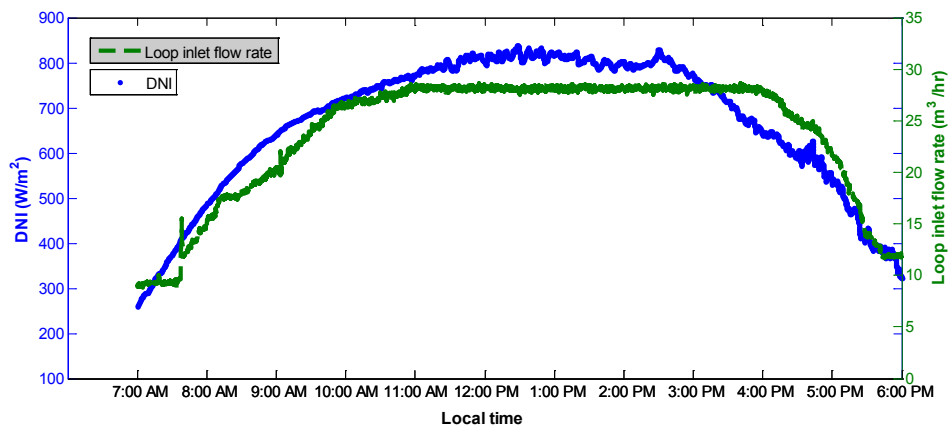


Fig. 8 Transient loop inlet flow rate (dashed line) and DNI (blue dot) on June 25, 2014 during 7am-6pm

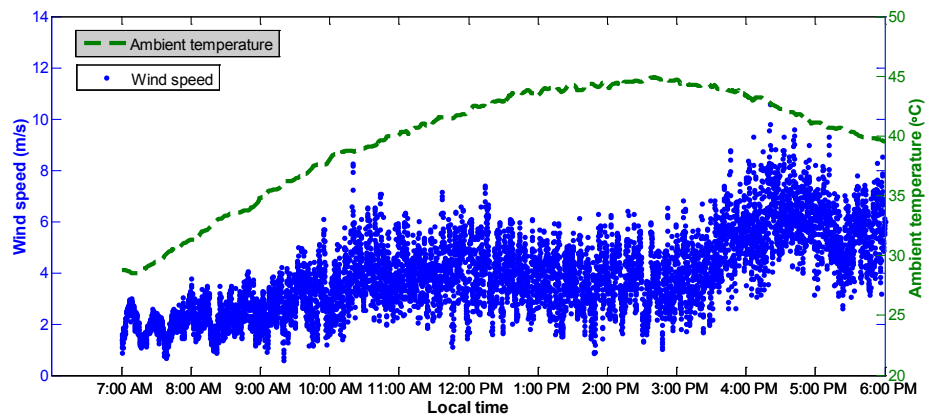


Fig. 9 Transient ambient temperature (dashed line) and wind speed (blue dots) on June 25, 2014 during 7am-6pm

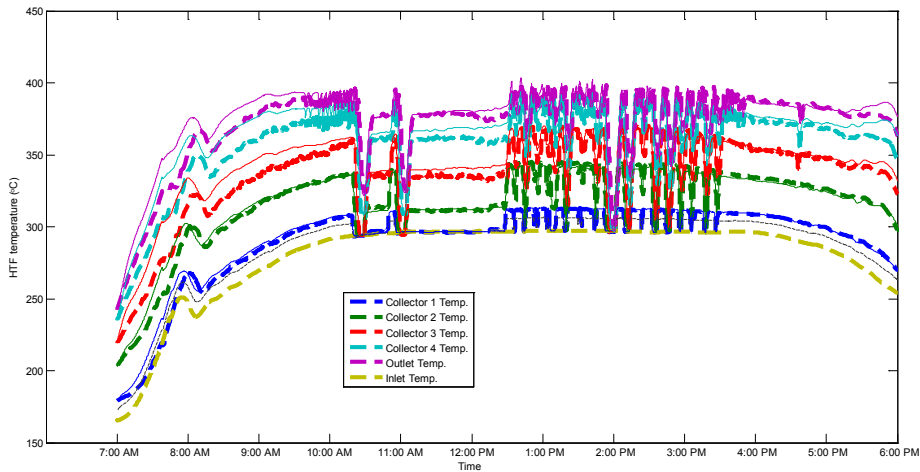


Fig. 10 Transient HTF Temperature and exit HTF temperature in Loop 1 on June 25, 2014 during 7am-6pm (thin solid line: model prediction; thick dashed line: measurement)

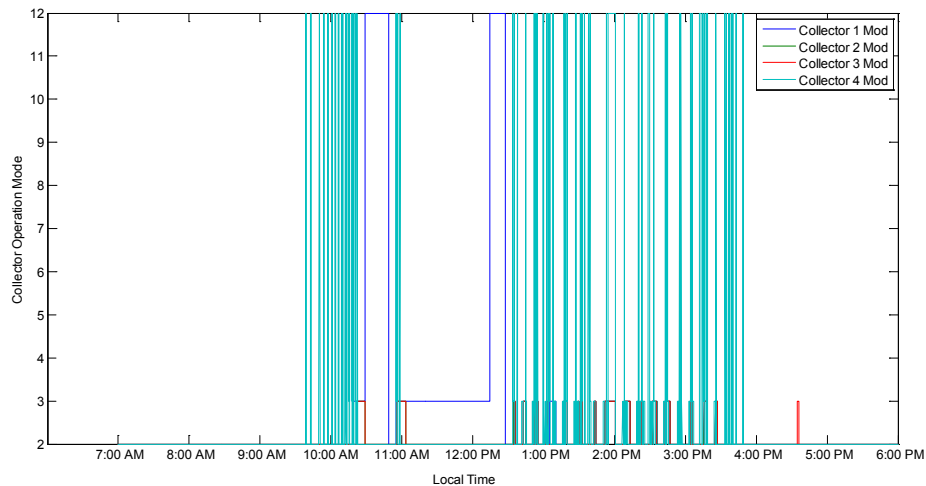


Fig. 11 Operation modes of solar collectors in Loop 1 on June 25, 2014 during 7am-6pm

Due to different cleaning status, local solar radiation and collector tracking conditions, the HTF oil flows exit from solar collector loops with different temperatures. The first-principle dynamic model in Eqs.(1.5)-(1.6) can characterize the influence of DNI, HTF inlet flow rate, wind speed, and ambient temperature on axial HTF temperature distribution in solar collector loops. As seen in Fig. 6-7 and Fig. 10, the proposed model can predict the HTF temperature change when collectors' operation modes vary from tracking to defocusing (Fig. 11). The model predictions show that the local HTF temperature is several degrees lower than the corresponding absorber surface temperature. The prediction of the loop exit HTF temperature generally agrees with the measurement, which demonstrated the predictive capability of our solar collector loop model. During the day, our prediction is slightly faster than real data especially for collector 3 and 4. This is because the current model ignores the fluid transport time in long connection pipes between collector 2 and 3 (Fig. 3) as well as the thermal inertia of insulated pipes. Significant modeling uncertainty during the start-up process may also come from the thermal inertia of the entire solar field, which was in cooled state on each early morning. We are investigating these effects systematically.

In some cases, the HTF exit temperature could approach to the high level (~ 400 °C). Safety control must be triggered to force the loop's collectors to partial out of focus (collectors' work mode from '2' to '12') until the HTF oil temperature gets down. Sometimes, the collector is even pushed to be totally defocused (collectors' work mode

from '12' to '3') for quick temperature drop (Fig. 12). Severe operation challenges have been observed in Fig. 13, where solar collectors swings frequently on a sunny day (higher DNI). This causes significant solar collection loss (Fig. 13). This is why advanced flow control strategies are needed to improve the operation safety and harvest more transient solar energy, particularly under nice weather conditions (Fig. 8).

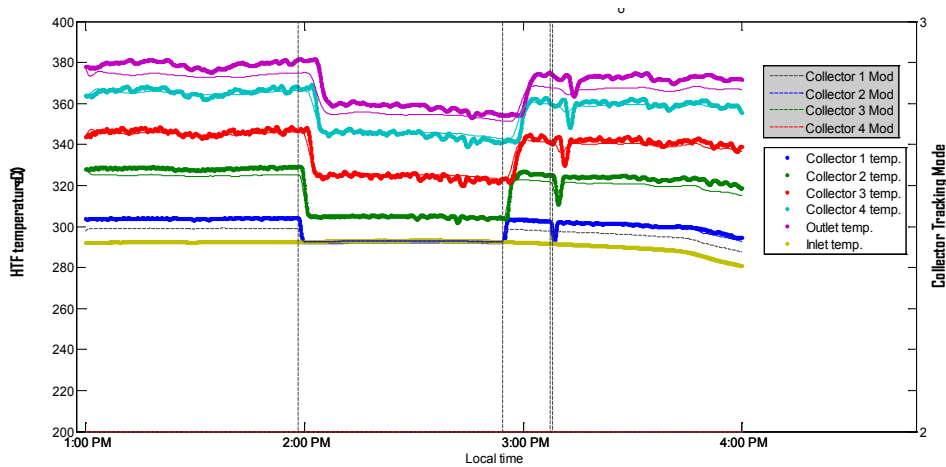


Fig. 12 Short-term transient Loop 1 HTF temperature, exit temperature and operation mode on June 24, 2014 (thin solid line: model prediction; thick dashed line: measurement)

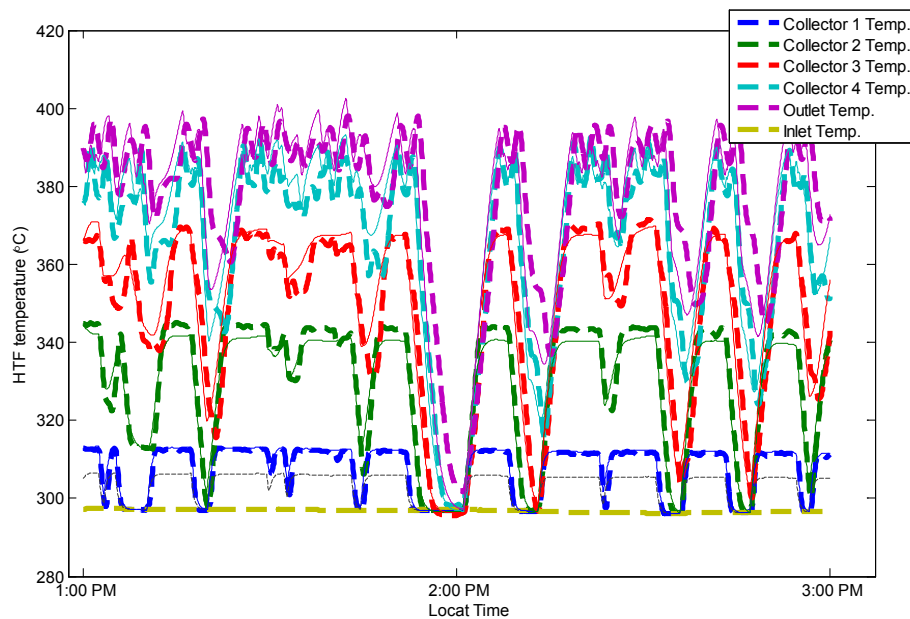


Fig. 13 Short-term transient HTF Temperature and exit temperature in Loop 1 on June 25, 2014 (thin solid line: model prediction; thick dashed line: measurement)

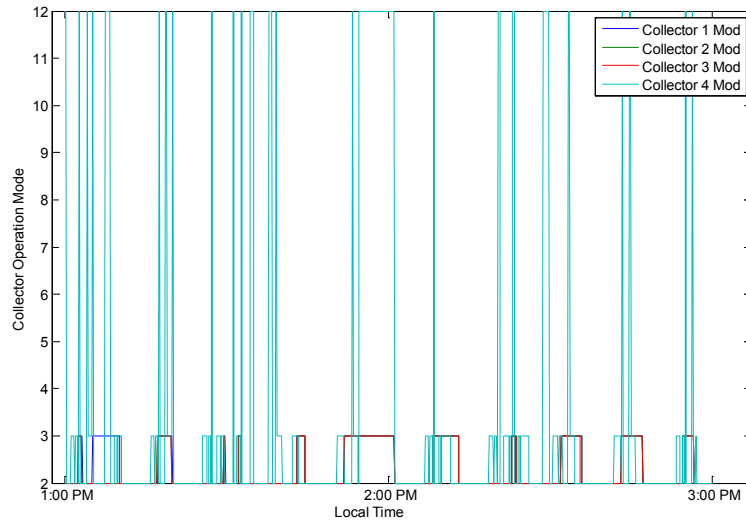


Fig. 14 Short term transient operation modes of four solar collectors in Loop 1 on June 25, 2014

4. Active HTF flow control

From the previous analysis, we have noticed that significant amount of solar energy is wasted during solar collector swinging in order to avoid HTF overheating. Moreover, fluctuating loop exit temperature also brings challenge to the operation of steam generator and turbine. The decentralized loop inlet valve may provide another option to control HTF overheating in local solar collectors. From the field data, the valve exhibit highly linear characteristics. Fig. 15 shows a step-up change in opening position of Loop 1 inlet valve, where the Loop 2 inlet valve and the total flow rate are kept constant. As expected, the loop 1 temperature is maintained within the limit (in Fig. 16) because the flow rate is increased. But the HTF flow rate in loop 2 would decrease and its temperature would exceed the limit. This is why the total HTF flow rate should also be increased by the pump so that the HTF fluid flow rate in Loop 2 would not drop (dotted-dash line in Fig. 15 instead of the dashed line).

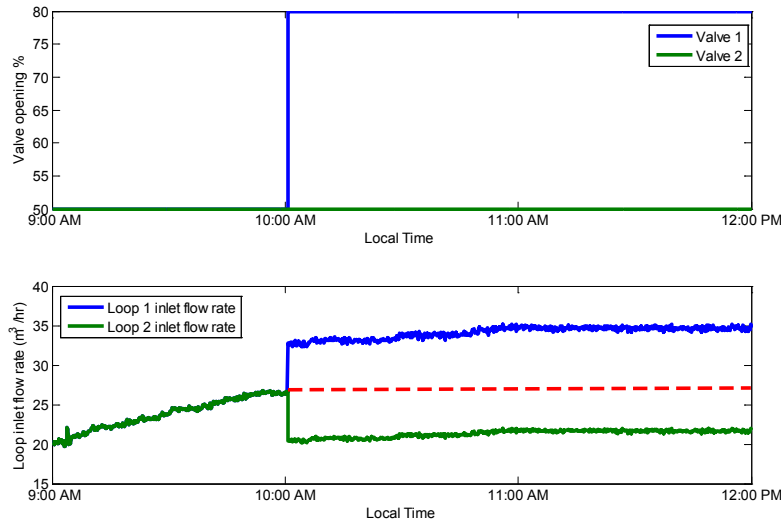


Fig. 15 Valve opening control in Loop 1 (red dashed line: compensated loop 2 flowrate)

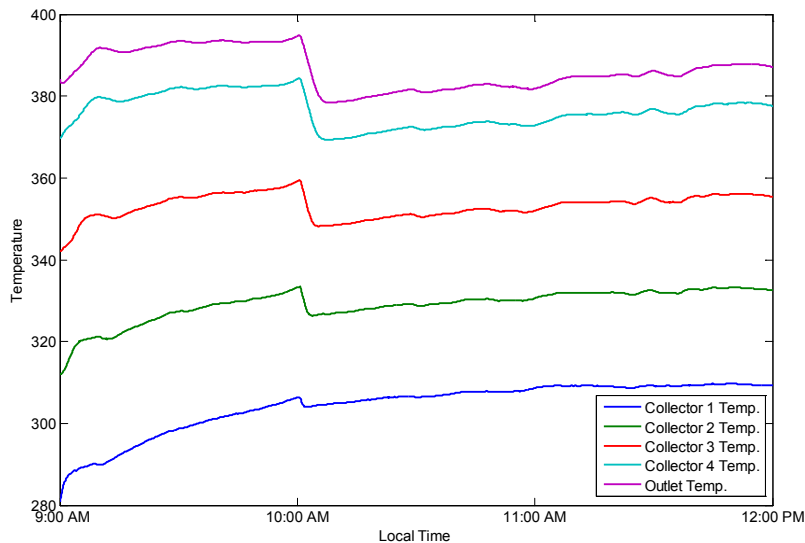


Fig. 16 Loop 1 HTF temperature responses to stepwise change of the first valve opening

5. Conclusions

A distributed first-principle model is developed to capture its transient characteristics of parabolic trough solar collector loops under variable solar irradiance, ambient temperature, wind speed, HTF inlet mass flow rate and temperature. The model predictions have showed good agreement with solar field data, which were collected from a 100 MW Shams 1 CSP plant in UAE. Based on initial evaluation of existing solar collectors' operation record, significant potential has been identified for solar energy harvesting. Coordinated loop inlet valve and overall pump control has been introduced to balance multiple solar collector loops at high HTF exit temperature for maximizing the power output of such a large-scale CSP plant.

Acknowledgements

This work is supported by the Cooperative Agreement between the Masdar Institute of Science and Technology (Masdar Institute), UAE and the Massachusetts Institute of Technology (MIT), USA. The authors would like to thank Mr. Alexander R. Higgs for his assistance to this work.

References

- [1] U. S. Department of Energy, *SunShot Vision Study*, 2012. http://www1.eere.energy.gov/solar/sunshot/vision_study.html
- [2] International Renewable Energy Agency, *Renewable Energy Technologies: Cost Analysis Series*, 2012.
- [3] D. Barlev, R. Vidu, and P. Stroeve, "Innovation in concentrated solar power," *Solar Energy Materials and Solar Cells*, vol. 95, pp. 2703-2725, 2011.
- [4] L. Roca, L.J. Yebra, et al., "Modeling of a solar seawater desalination plant for automatic operation purposes," *ASME Journal of Solar Energy Engineering*, vol. 130, 041009, 2008.
- [5] S.A. Kalogirou, "Solar thermal collectors and applications," *Progress in Energy and Combustion Science*, vol. 30, pp. 231-295, 2004.
- [6] E.F. Camacho, M. Berenguel, and F.R. Rubio, *Advanced Control of Solar Plants*, Springer, 1997.
- [7] T.A. Johansen and C. Storaas, "Energy-based control of a distributed solar collector field," *Automatica*, vol. 38, pp. 1191-1199, 2002.
- [8] L. Roca, M. Berenguel, et al., "Solar field control for desalination plants," *Solar Energy*, vol. 82, pp. 772-786, 2008.
- [9] F. Burkholder and C. F. Kutscher, *Heat loss testing of schott's 2008 PTR70 parabolic trough receiver*, U.S. National Renewable Energy Laboratory, 2009.
- [10] A.F. Mills, *Heat Transfer*, Prentice Hall PTR, 1999.